REVISIT OF TWO CLASSICAL ELASTICITY PROBLEMS BY USING THE NULL-FIELD BOUNDARY INTEGRAL EQUATIONS

J. T. Chen [*]

Department of Harbor and River Engineering
Department of Mechanical and Mechatronics Engineering
National Taiwan Ocean University
Keelung, Taiwan 20224, R.O.C.

Y. T. Lee [**]   **K. H. Chou** [***]

Department of Harbor and River Engineering
National Taiwan Ocean University
Keelung, Taiwan 20224, R.O.C.

ABSTRACT

In this paper, the two classical elasticity problems, Lamé problem and stress concentration factor, are revisited by using the null-field boundary integral equation (BIE). The null-field boundary integral formulation is utilized in conjunction with degenerate kernels and Fourier series. To fully utilize the circular geometry, the fundamental solutions and the boundary densities are expanded by using degenerate kernels and Fourier series, respectively. In the two classical problems of elasticity, the null-field BIE is employed to derive the exact solutions. The Kelvin solution is first separated to degenerate kernel in this paper. After employing the null-field BIE, not only the stress but also the displacement field are obtained at the same time. In a similar way, Lamé problem is solved without any difficulty.

Keywords : Degenerate kernel, Null-field boundary integral equation, Stress concentration factor, Lamé problem.

1. INTRODUCTION

Engineering problems are always simulated by using the mathematical models, *e.g.*, the steady state heat conduction problem [1], electrostatic potential [2] and torsion bar problems [3] are simulated by the Laplace equation; membrane vibration [4], acoustics [5] and water wave problems [6] are governed by the Helmholtz equation; plate vibration [7] and Stokes' flow [8] are formulated by the biharmonic equation. In order to solve boundary value problems, researchers and engineers have paid more attention on the development of boundary integral equation method (BIEM), boundary element method (BEM) and meshless method than domain type methods, finite element method (FEM) and finite difference method (FDM). Among various numerical methods, BEM is one of the most popular numerical approaches for solving boundary value problems. Although BEM has been involved as an alternative numerical method for solving engineering problems, some critical issues exist, *e.g.* singular and hypersingular integrals, boundary-layer effect, ill-posed system and mesh generation.

Unlike the conventional BEM and BIEM, Waterman [9] introduced first the so-called T-matrix method for electromagnetic scattering problems. Various names, null-field approach or extended boundary condition method (EBCM), have been coined from researchers of different fields. The null-field approach or T-matrix method was used widely for obtaining numerical solutions of acoustics [10], elastodynamics [11] and hydrodynamics [12]. Boström [13] introduced a new method of treating the scattering of transient fields by a bounded obstacle in the three-dimensional space. He defined new sets of time-dependent basis functions, and used these to expand the free space Green's function and the incoming and scattered fields. The method is a generalization to the time domain of the null-field approach first given by Waterman [9]. A crucial advantage of the null-field approach or T-matrix method consists in the fact that the influence matrix can be computed easily. Although many works for acoustic, elastodynamic and hydrodynamic problems have been done, only a few articles on elastostatics can be found

---

[*] Life-time Distinguished Professor, corresponding author   [**] Ph.D.   [***] Master student

[14]. The idea of changing the singularity distribution from real boundary to fictitious boundary (fictitious BEM) or putting the observation point outside the domain (null-field approach) can remove the singular and hypersingular integrals. However, they may result in an ill-posed matrix.

In the Fredholm integral equations, the degenerate kernel (or so-called separate kernel) plays an important role in mathematical analysis. Addition theorem may be better termed subtraction theorem to connect the degenerate kernel of two-point function of difference type in BEM implementation. However, its applications in practical problems seem to have taken a back seat to other methods. This degenerate kernel can be seen as one kind of approximation for fundamental solution, *i.e.*, the kernel function is expressed as finite sums of products by two linearly independent functions. The concept of generating "optimal" degenerate kernels has been proposed by Sloan *et al*. [15]. They also proved it to be equivalent to the iterated Petrov-Galerkin approximation. Later, Kress [16] proved that the integral equations of the second kind in conjunction with degenerate kernels have the convergence rate of exponential order instead of the linear algebraic order of conventional BEM. Recently, Chen *et al*. have successfully applied null-field integral equations in conjunction with degenerate kernels and Fourier series to solve Laplace [17], Helmholtz [18], biharmonic [19] and biHelmholtz [20] problems with circular holes. They claimed five advantages, (1) free of calculating principal values, (2) exponential convergence, (3) elimination of boundary-layer effect, (4) meshless, and (5) well-posed system, using the null-field approach. Following the success, they extended this approach to deal with inclusion problems [21]. In the approach, the calculation of principal value is avoided and the collocation exactly on the real boundary using the null-field formulation is achieved. They also found the rate of convergence of their approach is in the exponential order. Although they used the concept of null-field integral equation, we can locate the observer point exactly on the boundary in numerical implementation free of facing singularity thanks to the introduction of degenerate kernels.

It is well known that the degenerate scale occurs in the BEM or BIEM. For the Laplace problem, the mechanism of the degenerate scale was addressed by using the degenerate kernels. Also, the numerical work (using the boundary element method) and analytical study (using the method of stress function) for the degenerate scale in plane elasticity has been done. For more details on the degenerate scale in plane elasticity, readers may consult with the references [22,23].

In this paper, we develop a systematic approach to deal with elasticity problems with circular boundaries. The null-field integral formulation is utilized in conjunction with degenerate kernels and Fourier series. First, the Kelvin solution is expanded to the degenerate kernel. To fully utilize the circular geometry, the fundamental solutions and the boundary densities are expanded by using degenerate kernels and Fourier series, respectively. This approach is seen as a semi-analytical method for several circular holes, since the error stems from the truncation of Fourier series in the implementation. The advantages, free of calculating principal value, meshless and well-posed system are expected. For the circular and annular problems, the analytical solution can be obtained by using the present method. Finally, the two classical problems, one is an infinite plate with a circular hole subject to remote tension (stress concentration factor problem) and another is an annular cylinder subject to uniform pressures (Lamé problem), were given to see the validity of the present approach.

2. METHOD OF SOLUTION

2.1 Problem Statements

The two classical problems in the Timoshenko and Goodier's book [24] are revisted. One is an infinite plate with a circular hole subject to remote tension (stress concentration factor problem) and another is an annular cylinder subject to uniform pressures (Lamé problem) as shown in Figs. 1 and 2, respectively. The medium is considered as an isotropic, elastic and homogenous body. The governing equation is

$$(\lambda + G)\nabla(\nabla \cdot \underline{u}(x)) + G\nabla^2 \underline{u}(x) = 0 , \quad x \in \Omega , \quad (1)$$

where $\underline{u}(x)$ is the displacement, Ω is the domain of interest, ∇^2 is the Laplacian operator, and λ and G are the Lamé constants for the isotropic elasticity.

2.2 Dual Integral Formulation

The direct formulation of boundary integral equation method stems from the reciprocal work theorem. We have the Somigliana's identity [25],

$$u_j(s) = \int_B U_{ij}(x,s) \, t_i(x) \, dB(x) \\ - \int_B T_{ij}(x,s) \, u_i(x) \, dB(x) , \quad s \in \Omega , \quad (2)$$

$$0 = \int_B U_{ij}(x,s) \, t_i(x) \, dB(x) \\ - \int_B T_{ij}(x,s) \, u_i(x) \, dB(x) , \quad s \in \Omega^c , \quad (3)$$

where $U_{ij}(x, s)$ and $T_{ij}(x, s)$ are the Kelvin free-space Green's function of the *i*th direction response for displacement and traction, respectively, due to a concentrated load in the *j*th direction at the point *s*, and Ω^c denotes the complementary domain. Equations (2) and (3) can be changed to

$$u_i(x) = \int_B U_{ki}(s,x) \, t_k(s) \, dB(s) \\ - \int_B T_{ki}(s,x) \, u_k(s) \, dB(s) , \quad x \in \Omega , \quad (4)$$

$$0 = \int_B U_{ki}(s,x) \, t_k(s) \, dB(s) \\ - \int_B T_{ki}(s,x) \, u_k(s) \, dB(s) , \quad x \in \Omega^c , \quad (5)$$

The explicit form of $U_{ki}(s, x)$, or the so-called Kelvin solution, is
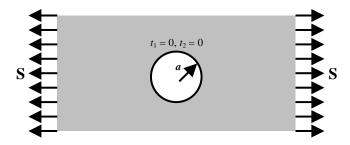
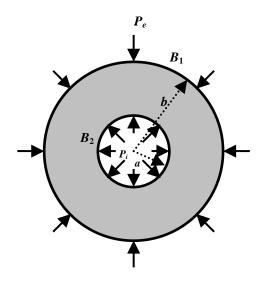Fig. 1 An infinite plate with a circular hole subject to remote tension

Fig. 2 An annular cylinder subject to uniform pressures

$$U_{ki}(s,x) = \frac{-1}{8\pi G(1-\nu)}\left((3-4\nu)\,\delta_{ki}\ln r - \frac{y_i\,y_k}{r^2}\right) \quad (6)$$

where ν is the Poisson ratio, $y_i = s_i - x_i$ and $i = 1, 2$ and $k = 1, 2$ for the plane elasticity. Now, in order to obtain an additional independent equation, we apply the traction operator [26] to Eqs. (4) and (5).Then, we have

$$t_p(x) = \int_B L_{kp}(s,x)\,t_k(s)\,dB(s)$$
$$-\int_B M_{kp}(s,x)\,u_k(s)\,dB(s)\ , \quad x\in\Omega\ , \quad (7)$$

$$0 = \int_B L_{kp}(s,x)\,t_k(s)\,dB(s)$$
$$-\int_B M_{kp}(s,x)\,u_k(s)\,dB(s)\ , \quad x\in\Omega^c\ , \quad (8)$$

Equations (4) and (7) are coined the dual boundary integral equations for the domain point and Eqs. (5) and (8) are called the dual null-field integral equations. When the field point x is collocated on the real boundary, the dual singular boundary integral equations for the boundary point ($x \in B$) can be obtained as follows:

$$c_{ij}\,u_j(x) = R.P.V.\int_B U_{ki}(s,x)\,t_k(s)\,dB(s)$$
$$-C.P.V.\int_B T_{ki}(s,x)\,u_k(s)\,dB(s)\ ,\ x\in B\ , \quad (9)$$

where $R.P.V.$ is the Riemann principal value, $C.P.V.$ is the Cauchy principal value, and c_{ij} is equal to $\delta_{ij} - B_{ij}$ in which B_{ij} depends on the solid angle of the corner at the boundary and on the Poisson ratio of the material of the body.   At a smooth boundary, B_{ij} reduces to $\delta_{ij}/2$.   By applying the traction operator to Eq. (9), we have

$$c_{pj}\,t_j(x) = C.P.V.\int_B L_{kp}(s,x)\,t_k(s)\,dB(s)$$
$$-H.P.V.\int_B M_{kp}(s,x)\,u_k(s)\,dB(s)\ ,\ x\in B\ , \quad (10)$$

where $H.P.V.$ denotes the Hadamard principal value. A detailed discussion for the dual boundary integral equations can be found in the original article by Hong and Chen [26] and a review article of Chen and Hong [27].   It is noted that the conventional null-field integral equations are not singular since s and x never coincide.   If the kernel functions in Eqs. (4), (5), (7) and (8) are substituted by using the appropriate degenerate (separable) kernels, we have

$$u_i(x) = \int_B U_{ki}(s,x)\,t_k(s)\,dB(s)$$
$$-\int_B T_{ki}(s,x)\,u_k(s)\,dB(s)\ , \quad x\in\Omega\cup B\ , \quad (11)$$

$$t_p(x) = \int_B L_{kp}(s,x)\,t_k(s)\,dB(s)$$
$$-\int_B M_{kp}(s,x)\,u_k(s)\,dB(s)\ , \quad x\in\Omega\cup B\ , \quad (12)$$

$$0 = \int_B U_{ki}(s,x)\,t_k(s)\,dB(s)$$
$$-\int_B T_{ki}(s,x)\,u_k(s)\,dB(s)\ , \quad x\in\Omega^c\cup B\ , \quad (13)$$

$$0 = \int_B L_{kp}(s,x)\,t_k(s)\,dB(s)$$
$$-\int_B M_{kp}(s,x)\,u_k(s)\,dB(s)\ , \quad x\in\Omega^c\cup B\ , \quad (14)$$

It is worth noting that kernels in Eqs. (11) ~ (12) and Eqs. (13) ~ (14) should be properly chosen to be the separable form.   According to Eqs. (11) ~ (14), the integral equations for the domain point or for the null-field point can include the collocation point on the real boundary since the appropriate degenerate kernels are used as will be elaborated on later.   Besides, the boundary integral equation is derived by using the bump contour approach in the conventional boundary element method.   Therefore, the free term c_{ij} appears. Here, we used the degenerate kernel instead of the closed-form fundamental solution.   We do not need to calculate the principal value by using the bump contour approach.   Therefore, c_{ij} disappears in our formulation when the collocation points are exactly located on the boundary.   For the non-smooth boundary, the degenerate kernel may be not available in the literature.   In other words, we may derive degenerate kernel by ourselves when the boundary is non-smooth.

2.3 Expansions of the Fundamental Solution and Boundary Density

   To fully utilize the property of circular geometry, the mathematical tools, separable kernel (or the so-called

degenerate kernel) and Fourier series, are utilized for an analytical study.

2.3.1 Degenerate (Separable) Kernel for the Fundamental Solution

In order to derive the degenerate kernel, the polar coordinates are utilized here. Therefore, the source and collocation points are expressed as (R, θ) and (ρ, ϕ), respectively, in the polar coordinate. The position vector of source point is $z_s = s_1 + s_2 i = Re^{i\theta}$. Similarly, the collocation point is $z_x = x_1 + x_2 i = \rho e^{i\phi}$. The former term $(\ln r)$ in the bracket of Eq. (6) is the fundamental solution of Laplace equation and the degenerate kernel can be found in [17].

In order to expand the term $(y_i y_k / r^2)$ in Eq. (6) into separable form, we have

$$
\frac{1}{z_x - z_s} = \frac{1}{(\rho\cos\phi + i\rho\sin\phi) - (R\cos\theta + iR\sin\theta)}
$$
$$
= \frac{(\rho\cos\phi - R\cos\theta) - i(\rho\sin\phi - R\sin\theta)}{\rho^2 + R^2 - 2R\rho\cos(\theta - \phi)}
$$
$$
= \frac{y_1 - iy_2}{r^2} , \tag{15}
$$

where $y_i = x_i - s_i$. For the exterior case $(R < \rho)$, Eq. (15) can be expanded as follows:

$$
\frac{1}{z_x - z_s} = \frac{1}{z_x} \frac{1}{1 - (z_s / z_x)}
$$
$$
= \frac{1}{z_x}\left[1 + \frac{z_s}{z_x} + \left(\frac{z_s}{z_x}\right)^2 + \left(\frac{z_s}{z_x}\right)^3 + \left(\frac{z_s}{z_x}\right)^4 + \cdots\cdots \right]
$$
$$
= \frac{1}{\rho} e^{-i\phi} \left[\sum_{m=0}^{\infty} \left(\frac{R}{\rho}\right)^m e^{im(\theta - \phi)} \right] . \tag{16}
$$

After comparing Eq. (15) with Eq. (16), we obtain

$$
\frac{y_1}{r^2} = \frac{\rho\cos\phi - R\cos\theta}{\rho^2 + R^2 - 2R\rho\cos(\theta - \phi)}
$$
$$
= \frac{1}{\rho}\sum_{m=0}^{\infty}\left(\frac{R}{\rho}\right)^m \cos[m\theta - (m+1)\phi] , \tag{17}
$$

$$
\frac{y_2}{r^2} = \frac{\rho\sin\phi - R\sin\theta}{\rho^2 + R^2 - 2R\rho\cos(\theta - \phi)}
$$
$$
= \frac{1}{\rho}\sum_{m=0}^{\infty}\left(\frac{R}{\rho}\right)^m \sin[m\theta - (m+1)\phi] . \tag{18}
$$

Then, we have

$$
\frac{y_1^2}{r^2} = \frac{1}{2} + \sum_{m=0}^{\infty}\frac{1}{2}\left(\frac{R}{\rho}\right)^m \cos[m\theta - (m+2)\phi]
$$
$$
- \sum_{m=0}^{\infty}\frac{1}{2}\left(\frac{R}{\rho}\right)^{m+1} \cos[(m-1)\theta - (m+1)\phi] , \tag{19}
$$

$$
\frac{y_2^2}{r^2} = \frac{1}{2} - \sum_{m=0}^{\infty}\frac{1}{2}\left(\frac{R}{\rho}\right)^m \cos[m\theta - (m+2)\phi]
$$
$$
+ \sum_{m=0}^{\infty}\frac{1}{2}\left(\frac{R}{\rho}\right)^{m+1} \cos[(m-1)\theta - (m+1)\phi] , \tag{20}
$$

$$
\frac{y_1 y_2}{r^2} = \frac{1}{2} + \sum_{m=0}^{\infty}\frac{1}{2}\left(\frac{R}{\rho}\right)^m \sin[m\theta - (m+2)\phi]
$$
$$
+ \sum_{m=0}^{\infty}\frac{1}{2}\left(\frac{R}{\rho}\right)^{m+1} \sin[(m-1)\theta - (m+1)\phi] , \tag{21}
$$

Similarly, we can obtain the separable form of terms of $y_i y_k / r^2$ for the interior case $(R > \rho)$ as shown below:

$$
\frac{y_1^2}{r^2} = \frac{1}{2} + \sum_{m=0}^{\infty}\frac{1}{2}\left(\frac{\rho}{R}\right)^m \cos[m\phi - (m+2)\theta]
$$
$$
- \sum_{m=0}^{\infty}\frac{1}{2}\left(\frac{\rho}{R}\right)^{m+1} \cos[(m-1)\phi - (m+1)\theta] , \tag{22}
$$

$$
\frac{y_2^2}{r^2} = \frac{1}{2} - \sum_{m=0}^{\infty}\frac{1}{2}\left(\frac{\rho}{R}\right)^m \cos[m\phi - (m+2)\theta]
$$
$$
+ \sum_{m=0}^{\infty}\frac{1}{2}\left(\frac{\rho}{R}\right)^{m+1} \cos[(m-1)\phi - (m+1)\theta] , \tag{23}
$$

$$
\frac{y_1 y_2}{r^2} = \frac{1}{2} + \sum_{m=0}^{\infty}\frac{1}{2}\left(\frac{\rho}{R}\right)^m \sin[m\phi - (m+2)\theta]
$$
$$
+ \sum_{m=0}^{\infty}\frac{1}{2}\left(\frac{\rho}{R}\right)^{m+1} \sin[(m-1)\phi - (m+1)\theta] , \tag{24}
$$

According to Eqs. (19) ~ (21) and (22) ~ (24), the degenerate kernel for the fundamental solution $U_{ki}(s, x)$, is obtained as

$$
U_{11}(s,x) = \begin{cases}
U_{11}^I(R,\theta\,;\,\rho,\phi) = -\dfrac{1}{8\pi G(1-\nu)}\left[(3-4\nu)\left(\ln R - \sum_{m=1}^{\infty}\dfrac{1}{m}\left(\dfrac{\rho}{R}\right)^m \cos(m(\theta-\phi)) \right) \right. \\
\left. -\dfrac{1}{2}\left(1 + \sum_{m=0}^{\infty}\left(\dfrac{\rho}{R}\right)^m \cos((m+2)\theta - m\phi) - \sum_{m=0}^{\infty}\left(\dfrac{\rho}{R}\right)^{m+1} \cos((m+1)\theta - (m-1)\phi) \right) \right] , \; R > \rho , \\[2ex]
U_{11}^E(R,\theta\,;\,\rho,\phi) = -\dfrac{1}{8\pi G(1-\nu)}\left[(3-4\nu)\left(\ln \rho - \sum_{m=1}^{\infty}\dfrac{1}{m}\left(\dfrac{R}{\rho}\right)^m \cos(m(\theta-\phi)) \right) \right. \\
\left. -\dfrac{1}{2}\left(1 + \sum_{m=0}^{\infty}\left(\dfrac{R}{\rho}\right)^m \cos(m\theta - (m+2)\phi) - \sum_{m=0}^{\infty}\left(\dfrac{R}{\rho}\right)^{m+1} \cos((m-1)\theta - (m+1)\phi) \right) \right] , \; R < \rho ,
\end{cases} \tag{25}
$$

$$U_{12}(s,x) = U_{21}(s,x) = \begin{cases} U_{12}^I(R,\theta\;;\rho,\phi) = \dfrac{1}{16\pi G(1-\nu)}\left(\sum_{m=0}^{\infty}\left(\dfrac{\rho}{R}\right)^m \sin\big((m+2)\,\theta - m\phi\big)\right. \\ \qquad\qquad \left. -\sum_{m=0}^{\infty}\left(\dfrac{\rho}{R}\right)^{m+1}\sin\big((m+1)\theta - (m-1)\,\phi\big)\right)\,,\ R>\rho\,, \\[2ex] U_{11}^E(R,\theta\;;\rho,\phi) = \dfrac{1}{16\pi G(1-\nu)}\left(\sum_{m=0}^{\infty}\left(\dfrac{R}{\rho}\right)^m \sin\big((m+2)\,\phi - m\theta\big)\right. \\ \qquad\qquad \left. -\sum_{m=0}^{\infty}\left(\dfrac{R}{\rho}\right)^{m+1}\sin\big((m+1)\,\phi - (m-1)\,\theta\big)\right)\,,\ R<\rho\,, \end{cases}$$

(26)

$$U_{22}(s,x) = \begin{cases} U_{22}^I(R,\theta\;;\rho,\phi) = -\dfrac{1}{8\pi G(1-\nu)}\left[(3-4\nu)\left(\ln R - \sum_{m=1}^{\infty}\dfrac{1}{m}\left(\dfrac{\rho}{R}\right)^m \cos\big(m(\theta-\phi)\big)\right)\right. \\ \qquad \left. -\dfrac{1}{2}\left(1+\sum_{m=0}^{\infty}\left(\dfrac{\rho}{R}\right)^m \cos\big((m+2)\,\theta - m\phi\big) + \sum_{m=0}^{\infty}\left(\dfrac{\rho}{R}\right)^{m+1}\cos\big((m+1)\,\theta - (m-1)\,\phi\big)\right)\right]\,,\ R>\rho\,, \\[2ex] U_{22}^E(R,\theta\;;\rho,\phi) = -\dfrac{1}{8\pi G(1-\nu)}\left[(3-4\nu)\left(\ln\rho - \sum_{m=1}^{\infty}\dfrac{1}{m}\left(\dfrac{R}{\rho}\right)^m \cos\big(m(\theta-\phi)\big)\right)\right. \\ \qquad \left. -\dfrac{1}{2}\left(1-\sum_{m=0}^{\infty}\left(\dfrac{R}{\rho}\right)^m \cos\big(m\theta - (m+2)\,\phi\big) + \sum_{m=0}^{\infty}\left(\dfrac{R}{\rho}\right)^{m+1}\cos\big((m-1)\,\theta - (m+1)\,\phi\big)\right)\right]\,,\ R<\rho\,, \end{cases}$$

(27)

and the three kernels $(T_{ki}(s,x)$, $L_{ki}(s,x)$ and $M_{ki}(s,x))$ can be obtained according to their definitions by using the traction operator in [26]. To the authors' best knowledge, the degenerate kernel for elasticity was not found in the literature before.

2.3.2 Fourier Series Expansion for Boundary Densities of Displacement and Traction

We apply the Fourier series expansion to approximate the boundary displacement u_k and traction t_k on the jth circular boundary,

$$u_k^j(s) = a_{0,k}^j + \sum_{n=1}^{\infty} a_{n,k}^j \cos n\theta_j + \sum_{n=1}^{\infty} b_{n,k}^j \sin n\theta_j\,,$$
$$s \in B_j\,,\ k = 1,2\,, \tag{28}$$

$$t_k^j(s) = p_{0,k}^j + \sum_{n=1}^{\infty} p_{n,k}^j \cos n\theta_j + \sum_{n=1}^{\infty} q_{n,k}^j \sin n\theta_j\,,$$
$$s \in B_j\,,\ k = 1,2\,, \tag{29}$$

where $a_{n,k}^j$, $b_{n,k}^j$, $p_{n,k}^j$ and $q_{n,k}^j$ $(k = 1, 2)$ are the Fourier coefficients and θ_j is the polar angle. In the real computation, only finite number of terms, M, is used for the Fourier series.

3. ILLUSTRATIVE EXAMPLES

The first example for verifying our formulation is an infinite plate with a circular hole subject to remote tension. Figure 1 shows an infinite plate with a circular

hole subject to a uniform tension of magnitude S in the x_1 direction. The radius of the hole is a. The problem can be decomposed into two parts by using the superposition technique as shown in Figs. 3(a) and 3(b). One is an infinite plate subject to a uniform tension and another is an infinite plate with a hole. On the boundary of the hole, it needs to satisfy the boundary conditions of free traction, $t_1 = 0$ and $t_2 = 0$, for the superposing total solution. According to the definition of traction, we obtain

$$t_1^{\infty} = \sigma_{11} \cdot n_1 + \sigma_{12} \cdot n_2 = -S\cos\theta \tag{30}$$

$$t_2^{\infty} = \sigma_{21} \cdot n_1 + \sigma_{22} \cdot n_2 = 0 \tag{31}$$

From the boundary conditions of free traction, the traction on the circular boundary in Fig. 3(b) is

$$t_1^h = S\cos\theta \tag{32}$$

$$t_2^h = 0 \tag{33}$$

By using Eq. (25), we have

$$0 = \int_B U_{11}^I(s,x)(S\cos\theta)\,dB(s)$$
$$- \int_B T_{11}^I(s,x)\left(a_{0,1}^h + \sum_{n=1}^{N} a_{n,1}^h \cos n\theta + \sum_{n=1}^{N} b_{n,1}^h \sin n\theta\right)dB(s)$$
$$- \int_B T_{21}^I(s,x)\left(a_{0,2}^h + \sum_{n=1}^{N} a_{n,2}^h \cos n\theta + \sum_{n=1}^{N} b_{n,2}^h \sin n\theta\right)dB(s)\,,$$

(34)
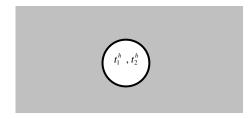
Fig. 3(a) An infinite plate subject to a uniform tension

Fig. 3(b)   An infinite plate with a hole

$$0 = \int_B U_{12}^I(s,x)(S\cos\theta) \, dB(s)$$
$$-\int_B T_{12}^I(s,x)\left(a_{0,1}^h + \sum_{n=1}^N a_{n,1}^h \cos n\theta + \sum_{n=1}^N b_{n,1}^h \sin n\theta\right) dB(s)$$
$$-\int_B T_{22}^I(s,x)\left(a_{0,2}^h + \sum_{n=1}^N a_{n,2}^h \cos n\theta + \sum_{n=1}^N b_{n,2}^h \sin n\theta\right) dB(s) ,$$

(35)

for the problem of an infinite plate with a hole in Fig. 3(b). The kernels, $U_{11}^I(s,x)$, $U_{12}^I(s,x)$, $T_{11}^I(s,x)$, $T_{12}^I(s,x)$, $T_{21}^I(s,x)$ and $T_{22}^I(s,x)$ can be substituted by using the separable forms in Eqs. (25) ~ (27). Through the procedure of comparing with the coefficients, we obtain

$$a_{1,1}^h = \frac{(1-\nu)\,Sa}{G} ,$$
$$a_{0,1}^h = a_{0,2}^h = a_{1,2}^h = a_{n,1}^h = a_{n,1}^h = 0 \quad (n = 2,\,3,\,\cdots) ,$$
$$b_{1,2}^h = -\frac{(1-2\nu)Sa}{2G} ,$$
$$b_{1,1}^h = b_{n,1}^h = b_{n,2}^h = 0 \quad (n = 2,\,3,\,\cdots) .$$

(36)

After determining the Fourier coefficients of boundary densities, the deformation fields are obtained by substituting the coefficients in Eq. (36) into Eq. (11).   The representations of displacement fields are

$$u_1^h(x) = \int_B U_{11}^E(s,x)(S\cos\theta) \, dB(s)$$
$$-\int_B T_{11}^E(s,x)\left(\frac{(1-\nu)\,aS}{G}\cos\theta\right) dB(s)$$
$$-\int_B T_{21}^E(s,x)\left(-\frac{(1-2\nu)\,aS}{2G}\sin\theta\right) dB(s) ,$$

(37)

and

$$u_2^h(x) = \int_B U_{12}^E(s,x)(S\cos\theta) \, dB(s)$$
$$-\int_B T_{12}^E(s,x)\left(\frac{(1-\nu)\,aS}{G}\cos\theta\right) dB(s)$$
$$-\int_B T_{22}^E(s,x)\left(-\frac{(1-2\nu)\,aS}{2G}\sin\theta\right) dB(s) .$$

(38)

After substituting the degenerate kernels, the deformation fields are obtained as follows:

$$u_1^h(x) = \frac{(1-\nu)\,S}{G}\frac{a^2}{\rho}\cos\phi + \frac{S}{4G}\frac{a^2}{\rho}\left(1-\frac{a^2}{\rho^2}\right)\cos 3\phi ,$$

(39)

$$u_2^h(x) = -\frac{(1-2\nu)\,S}{2G}\frac{a^2}{\rho}\sin\phi + \frac{S}{4G}\frac{a^2}{\rho}\left(1-\frac{a^2}{\rho^2}\right)\sin 3\phi .$$

(40)

For the other part solution in Fig. 3(a), it is simulated by using a circular plate with the radius b.   When the radius b approaches infinity, it is seen as an infinite plate.   Based on this concept, we obtain the Fourier coefficients as shown below:

$$a_{0,1}^\infty = a_{0,2}^\infty = arbitrary ,$$
$$b_{1,1}^\infty = -a_{1,2}^\infty$$
$$a_{1,1}^\infty = \frac{(1-\nu)Sb}{G} , \ a_{n,1}^\infty = a_{n,2}^\infty = 0 \ (n=2,\,3,\cdots) ,$$
$$b_{1,2}^\infty = -\frac{\nu Sb}{2G} , \ b_{n,1}^\infty = b_{n,2}^\infty = 0 \ (n=2,\,3,\,\cdots) .$$

(41)

After determining the Fourier coefficients of boundary densities, the deformation fields are obtained by substituting the coefficients in Eq. (41) into Eq. (11).   The coefficients, $a_{0,1}^\infty$, and $a_{0,2}^\infty$ are the rigid-body terms, and are set to zeros for simplicity.   The representations of deformation fields are

$$u_1^\infty(x) = \frac{(1-\nu)\,S\rho}{2G}\cos\phi + b_{1,1}^\infty\frac{\rho}{b}\sin\phi ,$$

(42)

$$u_2^\infty(x) = -\frac{\nu S\rho}{2G}\sin\phi - b_{1,1}^\infty\frac{\rho}{b}\cos\phi .$$

(43)

Although there is a free coefficient ($b_{1,1}^\infty$), it can be neglected for the near field since the outer radius b is infinity.   After determining the deformation fields for an infinite plate subject to a uniform tension and an infinite plate with a hole, the total deformation fields are

$$u_1 = \frac{(1-\nu)S}{G}\frac{a^2}{\rho}\cos\phi + \frac{S}{4G}\frac{a^2}{\rho}\left(1-\frac{a^2}{\rho^2}\right)\cos 3\phi + \frac{(1-\nu)S\rho}{2G}\cos\phi ,$$

(44)

$$u_2 = -\frac{(1-2\nu)S}{2G}\frac{a^2}{\rho}\sin\phi + \frac{S}{4G}\frac{a^2}{\rho}\left(1-\frac{a^2}{\rho^2}\right)\sin 3\phi - \frac{\nu S\rho}{2G}\sin\phi .$$

(45)

Based on the displacement fields, the stresses are easily obtained as

$$\sigma_{11} = \frac{\left[2\rho^4 - 3a^2\rho^2\cos 2\phi + a^2(3a^2 - 2\rho^2)\cos 4\phi\right]S}{\rho^4},$$

(46)

$$\sigma_{22} = \frac{\left[\rho^2\cos 2\phi + (3a^2 - 2\rho^2)\cos 4\phi\right]a^2 S}{2\rho^4}.$$

(47)

$$\sigma_{12} = \frac{\left[-\rho^2 + (6a^2 - 4\rho^2)\cos 2\phi\right]a^2 S}{2\rho^4}\sin 2\phi$$

(48)

By using the tensor transformation [24], the stresses in the polar coordinate can be represented as

$$\sigma_{rr} = \frac{(\rho^2 - a^2)\left[\rho^2 + (\rho^2 - 3a^2)\cos 2\phi\right]S}{2\rho^4},$$

(49)

$$\sigma_{\theta\theta} = \frac{\left[\rho^2(\rho^2 + a^2) - (\rho^4 + 3a^4)\cos 2\phi\right]S}{2\rho^4}.$$

(50)

$$\sigma_{r\theta} = \frac{(\rho^4 + 2a^2\rho^2 - 3a^4)S}{2\rho^4}\sin 2\phi$$

(51)

When $\rho = a$, Eqs. (49) ~ (51) are reduced to

$$\sigma_{rr} = 0,$$

(52)

$$\sigma_{\theta\theta} = S - 2S\cos 2\phi,$$

(53)

$$\sigma_{r\theta} = 0.$$

(54)

The hoop stress distribution in Eq. (53) is the same as that of Timoshenko and Goodier's book [24]. When ϕ is equal to $\pi/2$ or $3\pi/2$, the hoop stress ($\sigma_{\theta\theta}$) reaches the maximum of $3S$. However, it is not found for the displacement fields in the Timoshenko and Goodier's book [24]. Only the Airy stress function and stress were obtained in their book. If we would like to have the displacement fields, it is necessary to calculate the strain through the Hooke's law. Then, the displacement fields can be determined from the stress-strain relationship and integration of strain. The compatibility condition should be considered and the derivation is time-consuming. In the proposed approach, not only the stress but also the displacement fields can be directly obtained at the same time. In Fig. 4(a), it is obvious to observe that the plate is elongated uniformly in the x-axis direction since a uniform tension is given. The parameters of the material are given as $G = 1\text{N/m}^2$ and $v = 0.3$. The deformation in Fig. 4(b) occurs due to the boundary traction. Figure 4(c) shows the sketch of total deformation. Here, the magnitude S of the tension is one N/m^2, and the radius of the hole is one meter. It can be found that the circular hole is distorted. The same result can be obtained by using the *LM* hypersingular formulation of Eq. (14) as well as by using the *UT* singular formulation of Eq. (13). Two alternatives are provided in the proposed formulation.

The second example is an annular cylinder subject to uniform pressures (the Lamé problem). In this example,

Fig. 4(a) Deformation of an infinite plate subject to a uniform tension
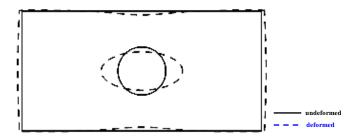

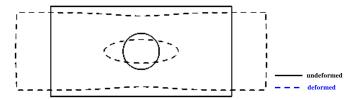Fig. 4(b) Deformation of an infinite plate with a hole

Fig. 4(c) Deformation of an infinite plate with a circular hole subject to remote tension

the problem subject to uniform pressures on the inner and outer surfaces is considered. Let a and b denote the inner and outer radii of the annular cylinder as shown in Fig. 2 where P_i and P_e are the uniform internal and external pressures, respectively. Then the boundary conditions are shown below:

$$(\sigma_{rr})_{r=a} = -P_i \text{ and } (\sigma_{rr})_{r=b} = -P_e.$$

(55)

This problem was first solved by Lamé [28]. Therefore, it is also called the Lamé problem. According to the definition of the traction, the boundary conditions of tractions are

$$t_1 = \sigma_{11} \cdot n_1 + \sigma_{12} \cdot n_2 = -P_e\cos\theta$$

(56)

$$t_2 = \sigma_{21} \cdot n_1 + \sigma_{22} \cdot n_2 = -P_e\sin\theta,$$

(57)

on the outer boundary B_1 and

$$t_1 = \sigma_{11} \cdot n_1 + \sigma_{12} \cdot n_2 = P_i\cos\theta$$

(58)

$$t_2 = \sigma_{21} \cdot n_2 + \sigma_{22} \cdot n_2 = P_i\sin\theta,$$

(59)

on the inner boundary B_2. The unknown boundary densities of displacement can be represented by using the Fourier series as

$$u_1 = a_0 + \sum_{n=1}^{N} a_n\cos n\theta + \sum_{n=1}^{N} b_n\sin n\theta$$

(60)

$$u_2 = \bar{a}_0 + \sum_{n=1}^{N} \bar{a}_n\cos n\theta + \sum_{n=1}^{N} \bar{b}_n\sin n\theta,$$

(61)

on B_1 and

$$u_1 = c_0 + \sum_{n=1}^{N} c_n \cos n\theta + \sum_{n=1}^{N} d_n \sin n\theta \qquad (62)$$

$$u_2 = \overline{c}_0 + \sum_{n=1}^{N} \overline{c}_n \cos n\theta + \sum_{n=1}^{N} \overline{d}_n \sin n\theta \ , \qquad (63)$$

on B_2. By using the null-field integral equation and Fourier series in Eq. (13), we obtain the Fourier coefficients as shown below:

$$a_0 = c_0 = arbitrary \ ,$$
$$\overline{a}_0 = \overline{c}_0 = arbitrary \ ,$$
$$b_1 = d_1 = -\overline{a}_1 = -\overline{c}_1 = arbitrary \ ,$$
$$a_1 = \overline{b}_1 = \frac{b\left[\left(a^2 + b^2(1-2\nu)\right)P_e - 2a^2(1-\nu)P_i\right]}{2(a^2 - b^2)\,G} \ ,$$
$$c_1 = \overline{d}_1 = \frac{a\left[2b^2(1-\nu)P_e - \left(b^2 + a^2(1-2\nu)\right)P_i\right]}{2(a^2 - b^2)\,G} \ ,$$
$$a_n = \overline{a}_n = b_n = \overline{b}_n = c_n = \overline{c}_n = d_n = \overline{d}_n = 0 \ \ (n = 2, 3, \cdots) \ .$$
$$(64)$$

After determining Fourier coefficients in Eq. (64), the deformation fields of Eq. (11) yield

$$u_1(\rho, \phi) = \frac{-(1-2\nu)\,P_e\,\rho}{4G(1-\nu)}\cos\phi + \frac{(1-2\nu)\,P_i}{4G(1-\nu)}\frac{a^2}{\rho}\cos\phi$$
$$+ a_1\frac{(1-2\nu)}{2(1-\nu)}\frac{\rho}{b}\cos\phi + c_1\frac{1}{2(1-\nu)}\frac{a}{\rho}\cos\phi$$
$$+ b_1\frac{\rho}{b}\sin\phi + a_0 \ , \ a < \rho < b \ , \ 0 \le \phi \le 2\pi \ , \quad (65)$$

$$u_2(\rho, \phi) = \frac{-(1-2\nu)\,P_e\,\rho}{4G(1-\nu)}\sin\phi + \frac{(1-2\nu)\,P_i}{4G(1-\nu)}\frac{a^2}{\rho}\sin\phi$$
$$+ a_1\frac{(1-2\nu)}{2(1-\nu)}\frac{\rho}{b}\sin\phi + c_1\frac{1}{2(1-\nu)}\frac{a}{\rho}\sin\phi$$
$$- b_1\frac{\rho}{b}\cos\phi + \overline{a}_0 \ , \ a < \rho < b \ , \ 0 \le \phi \le 2\pi \ . \quad (66)$$

In Eqs. (65) and (66), the coefficients (a_1 and c_1) are found in Eq. (64) and b_1 and $\overline{a}_0$ are arbitrary constants. The three terms ($b_1 \rho/b \cos\phi$, a_0 and $\overline{a}_0$) can be seen as rigid body terms of rotation and translation. The stresses are obtained as shown below:

$$\sigma_{rr}(\rho, \ \phi) = \frac{a^2 b^2 (P_0 - P_i) + (a^2 P_i - b^2 P_0)\,\rho^2}{(b^2 - a^2)\,\rho^2} \ ,$$
$$a < \rho < b \ , \ 0 \le \phi \le 2\pi \ , \qquad (67)$$

$$\sigma_{\theta\theta}(\rho, \ \phi) = \frac{a^2 b^2 (P_i - P_0) + (a^2 P_i - b^2 P_0)\,\rho^2}{(b^2 - a^2)\,\rho^2} \ ,$$
$$a < \rho < b \ , \ 0 \le \phi \le 2\pi \ , \qquad (68)$$

$$\sigma_{r\theta}(\rho, \ \phi) = 0 \ , \ a < \rho < b \ , \ 0 \le \phi \le 2\pi \ . \qquad (69)$$

For the special case of zero outer pressure $P_e = 0$, Eqs. (67) and (68) are reduced to

$$\sigma_{rr}(\rho, \ \phi) = \frac{a^2 P_i}{(b^2 - a^2)}\left(1 - \frac{b^2}{\rho^2}\right) \ , \ a < \rho < b \ , \ 0 \le \phi \le 2\pi \ ,$$
$$(70)$$

$$\sigma_{\theta\theta}(\rho, \ \phi) = \frac{a^2 P_i}{(b^2 - a^2)}\left(1 + \frac{b^2}{\rho^2}\right) \ , \ a < \rho < b \ , \ 0 \le \phi \le 2\pi \ .$$
$$(71)$$

These stress distributions are the same as those of Timoshenko and Goodier's solution [24]. As mentioned in the Example 1, only the Airy stress function is found in their book. For the proposed approach, the displacement fields and stress can be obtained at the same time. The inner and outer radii are given 1m and 5m, respectively. The uniform pressures are set as $P_e = 1\text{N/m}^2$ and $P_i = 2\text{N/m}^2$. The sketch of the deformation is shown in Fig. 5. Also, another alternative of the *LM* hypersingular formulation of Eq. (14) can be utilized to obtain the same result in the proposed approach. Here, we have proposed an alternative way to directly derive the exact solution of displacement and stress at the same time instead of using semi-inverse method. The two examples have been successfully used to verify the correctness of the degenerate kernels and the validity of our approach. For the problem with arbitrary number, different size and various locations of circular holes and/or inclusions in engineering practice, the results of torsion problems was published in [29]. However, the extension of the present approach to complex problems containing multiple holes and/or inclusions in plane elasticity deserves further study.
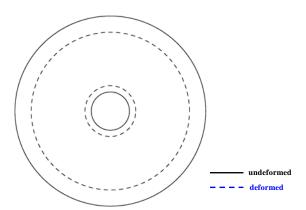

--- undeformed
- - - - deformed

Fig. 5 Deformation of an annular cylinder subject to uniform pressures

4. CONCLUDING REMARKS

For the elasticity problems with circular boundaries, we have proposed an analytical method by using the null-field integral formulation in conjunction with degenerate kernels and Fourier series. The Kelvin solution was expanded to degenerate kernel in this paper. Free of calculating principal value is our gain. Besides, displacement as well as stress responses were

both obtained at the same time. For the circular and annular cases, the analytical solutions for two illustrative examples, the stress concentration factor problem and the Lamé problem, were demonstrated to see the validity of the analytical formulation. Good agreements were made after comparing the results with those of Timoshenko and Goodier's textbook.

ACKNOWLEDGEMENTS

REFERENCES

1. Barone, M. R. and Caulk, D. A., "Optimal Arrangement of Holes in a Two-Dimensional Heat Conductor by a Special Boundary Integral Method," *International Journal for Numerical Methods in Engineering*, **18**, pp. 675−685 (1982).

2. Cheng, H. W. and Greengard, L., "On the Numerical Evaluation of Electrostatic Field in Dense Random Dispersions of Cylinders," *Journal for Computational Physics*, **136,** pp. 629−639 (1997).

3. Caulk, D. A., "Analysis of Elastic Torsion in a Bar with Circular Holes by a Special Boundary Integral Method," *Journal for Applied Mechanics*, ASME, **50**, pp. 101−108 (1983).

4. Hutchinson, J. R., *An Alternative BEM Formulation Applied to Membrane Vibrations*, Brebbia, C. A. and Maier, G. Eds., Boundary Elements VII, Springer-Verlag, Berlin (1985).

5. Chen, J. T. and Chen, K. H., "Dual Integral Formulation for Determining the Acoustic Modes of a Two-Dimensional Cavity with a Degenerate Boundary," *Engineering Analysis with Boundary Elements*, **21**, pp. 105−116 (1998).

6. Chen, K. H., Chen, J. T., Chou, C. R. and Yueh, C. Y., "Dual Boundary Element Analysis of Oblique Incident Wave Passing a Thin Submerged Breakwater," *Engineering Analysis with Boundary Elements*, **26,** pp. 917−928 (2002).

7. Hutchinson, J. R., *Vibration of Plates*, Brebbia, C. A. Ed., Boundary Elements X, Springer-Verlag, Berlin (1988).

8. Mills, R. D., "Computing Internal Viscous Flow Problems for the Circle by Integral Methods," *Journal for Fluid Mechanics*, **73**, pp. 609−624 (1977).

9. Waterman, P. C., "Matrix Formulation of Electromagnetic Scattering," *Proceedings of the Institute of Electrical and Electronics Engineers*, **53**, pp. 805−812 (1965).

10. Bates, R. H. T., "Modal Expansions for Electromagnetic Scattering From Perfectly Conducting Cylinders of Arbitrary Cross-Section," *Proceedings of the Institution of Electrical Engineers,* **115**, pp. 1443−1445 (1968).

11. Waterman, P. C., "Matrix Theory of Elastic Wave Scattering," *Journal of the Acoustical Society of America*, **60**, pp. 567−580 (1967).

12. Martin, P. A., "On the Null-Field Equations for Water-Wave Radiation Problems," *Journal of Fluid Mechanics*, **113,** pp. 315−332 (1981).

13. Boström, A., "Time-Dependent Scattering by a Bounded Obstacle in Three Dimensions," *Journal of Mathematical Physics,* **23**, pp. 1444−1450 (1982).

14. Olsson, P., "Elastostatics as a Limit of Elastodynamics—A Matrix Formulation," *Applied Scientific Research,* **41**, pp. 125−151 (1984).

15. Sloan, I. H., Burn, B. J. and Datyner, N., "A New Approach to the Numerical Solution of Integral Equations," *Journal of Computational Physics*, **18**, pp. 92−105 (1975).

16. Chen, J. T. and Hong, H.-K., "Dual Boundary Integral Equations at a Corner Using Contour Approach Around Singularity," *Advances in Engineering Software*, **21**, pp. 169−178 (1994).

17. Chen, J. T., Shen, W. C. and Wu, A. C., "Null-Field Integral Equations for Stress Field Around Circular Holes Under Anti-Plane Shear," *Engineering Analysis with Boundary Elements*, **30**, pp. 205−217 (2005).

18. Chen, J. T., Chen, C. T., Chen, P. Y. and Chen, I. L., "A Semi-Analytical Approach for Radiation and Scattering Problems with Circular Boundaries," *Computer Methods in Applied Mechanics and Engineering*, **196**, pp. 2751−2764 (2007).

19. Chen, J. T., Hsiao, C. C. and Leu, S. Y., "Null-Field Integral Equation Approach for Plate Problems with Circular Boundaries," *Journal for Applied Mechanics,* ASME, **73**, pp. 679−693 (2006).

20. Lee, W. M., Chen, J. T. and Lee, Y. T., "Free Vibration Analysis of Circular Plates with Multiple Circular Holes Using Indirect BiEMs," *Journal for Sound and Vibration*, **304**, pp. 811−830 (2007).

21. Chen, J. T. and Wu, A. C., "Null-Field Approach for the Multi-Inclusion Problem Under Anti-Plane Shears," *Journal for Applied Mechanics*, ASME, **74**, pp. 469−487 (2007).

22. Chen, J. T., Kuo, S. R. and Lin, J. H., "Analytical Study and Numerical Experiments for Degenerate Scale Problems in the Boundary Element Method for Two-Dimensional Elasticity," *International Journal for Numerical Methods in Engineering,* **54**, pp. 1669−1681 (2002).

23. Chen, J. T., Lin, S. R. and Chen, K. H., "Degenerate Scale Problem when Solving Laplace's Equation by BEM and its Treatment," *International Journal for Numerical Methods in Engineering*, **62**, pp. 233−261 (2005).

24. Timoshenko, S. P. and Goodier, J. N., *Theory of Elasticity*, McGraw-Hill, New York (1970).

25. Banerjee, P. K. and Butterfield, R., *Boundary Element Method in Engineering Science*, McGraw-Hill, New York (1981).

26. Hong, H.-K. and Chen, J. T., "Derivations of Integral Equations of Elasticity," *Journal for Engineering Mechanics*, ASCE, **114**, pp. 1028−1044 (1988).

27. Chen, J. T. and Hong, H.-K., "Review of Dual Boundary Element Methods with Emphasis on Hypersingular Integrals and Divergent Series," *Applied Mechanics Reviews*, ASME, **52**, pp. 17−33 (1999).

28. Lamé, G., *Leçons Sur La Théorie De L'Élasticité*, Gauthier-Villars, Paris (1852).

29. Chen, J. T and Lee, Y. T., "Torsional Rigidity of a Circular Bar with Multiple Circular Inclusions Using the Null-Field Integral Approach," *Computational Mechanics*, **44**, pp. 221−232 (2009).